600 and 800 cm^{-1}. No evidence for either band was obtained. Moreover, the evidence suggests strongly that the H-Cl bond was not ruptured and that hydrogen-bond formation instead occurred. Finally, the protonation reaction would have given rise to ionic (ion pair) products; these have only rarely been observed in matrices for Bronsted acid/base pairs and are disfavored by the very nonpolar nature of the argon matrix.

The slow warm-up experiments provide some additional evidence for hydrogen-bond formation. At 41 K, the argon matrix is very slushy, and diffusion can occur to increase the yield of the isolated 1/1 complex, as observed. By 59 K, the argon matrix material was vaporizing, leaving behind both unreacted HCl and Cp_2TiF_2 as well as product. Since there is likely no barrier to complex formation, all of the Cp_2TiF_2 reacted, leaving no parent Cp_2TiF_2. The strong absorptions at 520 and 831 cm^{-1} indicate that aggregation had occurred by this temperature, and the isolated 1/1 complex was no longer present. However, since HCl was present in excess, some residual $(HCl)_x$ was observed. By 122 K, all of the residual $(HCl)_x$ had vaporized and been pumped off, but the HCl bound to Cp_2TiF_2 remained. By 157 K, the aggregated complex had dissociated and the HCl vaporized and pumped off, leaving behind a thin film of Cp_2TiF_2. It is interesting that the HCl stretching mode shifted to higher energy upon warming and aggregation, from approximately 2440 to 2550 cm^{-1} near 60 K. A smaller red shift is generally interpreted to mean a weaker interaction,[20] which suggests that the hydrogen-bonded HCl molecules in the aggregate are less strongly bound than the single HCl in the 1/1 complex. One explanation is that the 1/1 complex is bidentate and upon aggregation a monodentate 2/1 complex is formed (one HCl with each fluorine). However, given the large bandwidths of these bands, this must be regarded as tentative. The slow warm-up sequence with Cp_2TiCl_2 gave quite similar results, with initially increased product formation and then shifting and broadening of the product absorption, before decomposition of the product. It is noteworthy that, at 122 K, most of the Cp_2TiCl_2·HCl complex had dissociated, while, at the same temperature, most of the Cp_2TiF_2·HCl complex remained, suggesting stronger binding in the latter complex. This conclusion must be tempered by the fact that the warm-up process was continuous taking between 20 and 60 s for the temperature to increase by one degree, so that it is possible that slow processes might not have reached equilibrium at a given temperature (kinetic rather than thermodynamic control). In this case, comparing the temperatures needed for decomposition would not be valid.

The halogen-exchange reaction between Cp_2TiF_2 and HCl to yield Cp_2TiClF and HF is known to occur in solution[22] and might occur during the slow warm-up experiments conducted here. However, monomeric HF absorbs near 3940 cm^{-1} and was not observed. If the HF product were hydrogen bonded to the Ti-Cl or Ti-F bond, then a distinct absorption red shifted from 3940 cm^{-1} should have been observed and was not. Also, no perceptible decrease in the Ti-F absorptions was seen, indicating little if any reaction. Consequently, there is no evidence that the halogen-exchange reaction occurred under these experimental conditions. Of course, the reaction would have had to occur prior to the decomposition of the complex and vaporization of the HCl, which took place between 122 and 157 K.

Acknowledgment. The National Science Foundation is gratefully acknowledged for support of this research through Grant CHE 87-21969. Professor Tom Richmond is gratefully acknowledged for supplying samples of the titanocene dihalides, as well as for helpful discussions and providing results prior to publication.

(22) Richmond, T. G. Private communication.

Contribution from the Chemistry Department, University of California, Davis, California 95616

Synthesis and Structural Characterization of Manganese(II) Derivatives of the Bulky, Chelating Bis(amido) Ligands $[(NMes)_2SiMe_2]^{2-}$ and $[DippNCH_2CH_2NDipp]^{2-}$, Their Neutral Amine Precursors, and Their Lithium Salts (Mes = 2,4,6-$Me_3C_6H_2$; Dipp = 2,6-*i*-$Pr_2C_6H_3$)

Hong Chen, Ruth A. Bartlett, H. V. Rasika Dias, Marilyn M. Olmstead, and Philip P. Power*

Received October 29, 1990

The synthesis of three new bulky bidentate diamines, the compounds $Me_2Si(NHMes)_2$ (**1**), Mes(H)NCH_2CH_2N(H)Mes (**2**) (Mes = 2,4,6-$Me_3C_6H_2$), and Dipp(H)NCH_2CH_2N(H)Dipp (**3**) (Dipp = 2,6-i-$Pr_2C_6H_3$ is described. The addition of 2 equiv of *n*-BuLi to **1** or **3** results in almost quantitative yields of the novel dimeric solvent-free dilithium derivatives $[\{Li(Mes)N\}_2SiMe_2]_2$ (**4**) and $[Li(Dipp)NCH_2CH_2N(Dipp)Li]_2$ (**5**). The reaction of **1** with $Mn\{N(SiMe_3)_2\}_2$ in the presence of $LiN(SiMe_3)_2$ gives the unusual product $[Li(Mn\{NMes\}_2SiMe_2)_2N(SiMe_3)_2]$ (**6**), which features a dimeric Mn salt of the dianion of **1** and, in addition, a Li^+ ion sandwiched between two mesityl rings. The reaction of the bulky amine **3** affords the monomeric manganese(II) amide Mn[N-(Dipp)CH_2CH_2N(H)Dipp]$_2$ (**7**), which has a very distorted geometry at Mn as a result of the steric requirements and bonding of ligand **3**. Compounds **1** and **3**-**7** have been characterized by X-ray crystallography. Crystallographic data with Cu Kα radiation (λ = 1.541 78 Å) for **1** and **4**-**6** and Mo Kα radiation (λ = 0.710 69 Å) for **3** and **7** at 130 K: **1**, a = 16.401 (10) Å, b = 6.386 (2) Å, c = 9.244 (2) Å, Z = 2, orthorhombic, space group $P2_12_12$: **3**, a = 10.968 (3) Å, b = 11.859 (4) Å, c = 20.455 (7) Å, α = 93.61 (3)°, β = 103.41 (3)°, γ = 109.22 (3)°, Z = 4, triclinic, space group $P\bar{1}$; **4**, a = 9.360 (3) Å, b = 10.052 (2) Å, c = 11.313 (3) Å, α = 77.08 (2)°, β = 85.49 (2)°, γ = 73.50 (2)°, Z = 1, triclinic, space group $P\bar{1}$; **5**, a = 12.758 (4) Å, b = 12.828 (5) Å, c = 19.085 (8) Å, β = 103.23 (3)°, Z = 4, monoclinic, space group $P2_1/c$; **6**, a = 12.918 (5) Å, b = 14.552 (5) Å, c = 13.395 (6) Å, β = 90.35 (3)°, Z = 2, monoclinic, space group $P2_1$: **7**, a = 21.713 (12) Å, b = 13.927 (6) Å, c = 17.764 (11) Å, β = 117.51 (4)°, Z = 4, monoclinic, space group $C2/c$.

Introduction

Amide ($-NR_2$) derivatives of the transition metals are an interesting and varied class of compounds that exhibit a very broad range of structures and reaction types.[1] The combination of high M-N bond strength and steric flexibility has ensured that these ligands have played a pioneering role in the synthesis of numerous low- (two- or three-) coordinate transition-metal complexes.[2,3] In many instances, amide complexes have provided the first examples of these unusual transition-metal coordination numbers.[4] In

(1) Lappert, M. F.; Power, P. P.; Sanger, A. R.; Srivastava, R. C. *Metal and Metalloid Amides*; Ellis Horwood: Chichester, England 1980.

(2) Bradley, D. C. *Chem. Br.* **1975**, *11*, 393. Bradley, D. C.; Chisholm, M. H. *Acc. Chem. Res.* **1976**, *9*, 273.

(3) Eller, P. G.; Bradley, D. C.; Hursthouse, M. B.; Meek, D. W. *Coord. Chem. Rev.* **1977**, *24*, 1.

0020-1669/91/1330-2487$02.50/0

addition, amide derivatives have proved extremely useful as starting materials for the preparation of other transition-metal species.

In spite of the impressive body of information now known, little work has appeared on saturated multidentate amide ligands that feature two or more amide bonding centers. With the exception of porphyrin and related cyclic derivatives, which constitute a specialized class of delocalized amide ligand, there are only a handful of reports of well-characterized multidentate amide complexes in the literature. Much of the work on these concerns elements of the titanium group in their highest oxidation state (+4), and some have been structurally characterized.[1,5] In addition, some Ti derivatives of the saturated, cyclic, multidentate ligand cyclam have appeared.[6] Work in the main-group elements has shown that complexes of multidentate amide ligands such as $[\{N(t\text{-}Bu)\}_2SiMe_2]^{2-}$ and related species have an interesting and rich chemistry.[7] In addition, recent work on the related $[\{N(t\text{-}Bu)\}_2BPh]^{2-}$[8] and benzamidinato, $[(NR)_2CPh]^-$,[9] ligands has resulted in the synthesis of a number of main-group and lanthanide derivatives. Other relevant work has involved the interesting 1,4-diazabutadiene ligands (RNCHCHNR). The use of these ligands has permitted the isolation and characterization of several new metal complexes of unusual structure.[10] In this laboratory, some recent work has focused on the synthesis, characterization, and chemistry of low-coordinate transition-metal amides, and this has resulted in the isolation and structural determination of several two-coordinate complexes whose chemistry is currently under investigation.[11-13] This work has led to the suggestion that the synthesis of complexes derived from sterically demanding bis(amido) ligands might lead to species of unusual structure in which two low-coordinate metal centers are held in close proximity. The initial results derived from these studies are now described in this paper.

Experimental Section

General Procedures. All reactions were performed by using modified Schlenk techniques under an inert atmosphere of N_2 or a Vacuum Atmospheres HE43-2 drybox. Solvents were freshly distilled under N_2 from Na/K or sodium/potassium benzophenone ketyl and degassed twice immediately before use. ^1H NMR spectra were obtained on a General Electric QE-300 NMR spectrometer and referenced to TMS. Magnetic moment measurements were performed via Evans' method.[14] Compounds **1-7** gave satisfactory analyses for C, H, and N. Me_2SiCl_2 and the solution of 1.6 M *n*-BuLi in hexane were used as received. Ethylene dibromide, 2,6-diisopropylaniline ($DippNH_2$), and mesitylamine were distilled off drying agents (P_2O_5 or CaH_2) before use. $Mn[N(SiMe_3)_2]_2$ was synthesized via a slight modification of the literature procedure.[15]

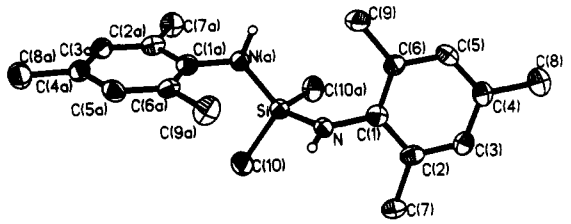

Figure 1. Thermal ellipsoidal plot of $Me_2Si(NHMes)_2$ (**1**). H atoms (except N H's) are omitted for clarity.

Syntheses of Compounds 1-7. $Me_2Si(NHMes)_2$ (1). H_2NMes (2.70 g, 20 mmol) in Et_2O (50 mL), cooled in an ice bath, was treated dropwise with *n*-BuLi (12.88 mL, 1.6 M hexane solution). A white precipitate formed immediately after the addition was completed. The solution was allowed to warm to room temperature, and it was stirred further for 1 h. Then, Me_2SiCl_2 (1.29 g, 10 mmol) was added dropwise by using a syringe. The solution was then stirred overnight, and the volatile material was removed by reduced pressure. The residue was extracted with pentane (50 mL), and the solution was filtered. Reduction of the filtrate volume to ca. 10 mL, followed by cooling overnight in a −20 °C freezer, afforded **1** as colorless crystals. Yield = 2.29 g, 70%; mp = 65–66 °C. ^1H NMR ($CDCl_3$): δ 0.18 (s, 6 H, 2 Me), 2.22, 2.23 (2 s, 18 H, *o*- and *p*-CH_3), 2.64 (s, 2 H, NH), 6.83 (s, 4 H, phenyl H)].

MesN(H)CH_2CH_2(H)NMes (2) and DippN(H)CH_2CH_2(H)NDipp (3) (Dipp = 2,6-*i*-$Pr_2C_6H_3$). A detailed description of the synthesis of **3** is provided. Compound **2** was synthesized in a similar manner by the reaction of 66.7 g of $MesNH_2$ and 15.4 g of ethylene dibromide. H_2NDipp (210 g, 1.18 mol) was placed in a 500-mL three-neck flask, and ethylene dibromide (33.70 g, 0.18 mol) was added dropwise at room temperature. This mixture was stirred for 10 min and then heated at 120 °C for 2 days. The excess amine (ca. 103 g, which can be reused) was distilled off under reduced pressure, and the residue was allowed to react with finely divided KOH (28 g, 0.50 mol) at 100 °C for 5 h. This mixture was filtered, and the solid was washed with Et_2O (3 × 50 mL). The combined filtrate was distilled to remove unreacted H_2NDipp and Et_2O. The viscous oil was dissolved in methanol, and product **3** crystallized as colorless crystals after the methanol solution was cooled in a −20 °C freezer overnight. Yield = 33 g, 48%; mp = 98–100 °C. ^1H NMR (C_6D_6): δ 1.20 (d, 24 H, isopropyl CH_3), 3.18 (s, 4 H, CH_2CH_2), 3.38 (m, 4 H, isopropyl CH), 3.40 (s, 2 H, NH), 7.13 (m, 6 H, phenyl H)]. The yield for **2** was ~6 g, 25%; mp = 34–36 °C. ^1H NMR ($CDCl_3$): δ 2.24, 2.22 (2 s, 18 H, *o*- and *p*-CH_3), 3.2 (s, 4 H, CH_2CH_2), 3.38 (s, 2 H, NH), 7.1 (s, 4 H, *m*-H).

[{Li(Mes)N}$_2$$SiMe_2$]$_2$ (4). {Mes(H)N}$_2$$SiMe_2$ (1.31 g, 4 mmol) in hexane (20 mL) was treated dropwise with *n*-BuLi (5.15 mL, 1.6 M hexane solution). A white precipitate of **4** was formed immediately. The solution was stirred for 2 h whereupon the volatile material was removed under reduced pressure. The white residue was redissolved in ca. 10 mL of warm (40 °C) toluene. Hexane (~10 mL) was added to produce incipient crystallization. Filtration followed by cooling for 12 h in a −20 °C freezer afforded **4** in almost quantitative yield; mp = 280 °C.

[Li(Dipp)NCH_2CH_2N(Dipp)Li]$_2$ (5). Diamine **3** (0.71 g) was dissolved in hexane (50 mL). A 2.4-mL aliquot of a 1.6 M *n*-BuLi/hexane solution was added dropwise, and the solution was stirred for 4 h. Filtration followed by cooling overnight in a −20 °C afforded the product **5** as colorless crystals. Yield = 0.55 g, 70%; the compound softens at ~155 °C and melts to an orange liquid at 188–192 °C.

[Li(Mn[NMes]$_2$$SiMe_2$)$_2$N($SiMe_3$)$_2$] (6). $Mn[N(SiMe_3)_2]_2$ (0.75 g, 2 mmol), $Me_2Si(NHMes)_2$ (0.65 g, 2 mmol), and $LiN(SiMe_3)_2$ (0.17 g, 1 mmol) were heated together at 90 °C in a Schlenk tube. The mixture became red upon heating for 1 h. The volatile byproduct $HN(SiMe_3)_2$ was removed under reduced pressure, which produced concomitant solidification of the residue. The solid was extracted with hexane (20 mL), and the solution was filtered. The volume was then reduced to ca. 10 mL under reduced pressure. Cooling overnight in a −20 °C freezer gave the product (**5**) as pale, canary yellow crystals. Yield = 0.51 g, 55%; mp = 200 °C dec; $\mu = 2.9\ \mu_B$.

Mn[N(Dipp)CH_2CH_2N(H)Dipp]$_2$ (7). $Mn[N(SiMe_3)_2]_2$ (0.38 g, 1 mmol) and **3** (0.76 g, 2 mmol) were heated together to 100 °C for 1 h. The mixture became dark red, and the volatile material was then removed under reduced pressure. Extraction of the dark red residue with hexane (30 mL), filtration, and reduction of the volume to 20 mL afforded the product **7** as red crystals. Yield = 0.163 g, 20%; mp = 185–190 °C. UV-vis: 18 050 cm^{-1} (ε = 160), 23 700 cm^{-1} (ε = 420). $\mu = 5.9\ \mu_B$.

(4) Recent examples are the first instances of three-coordinate Mn(III) and Co(III): Ellison, J. J.; Power, P. P.; Shoner, S. C. *J. Am. Chem. Soc.* **1989**, *111*, 8044.
(5) Bürger, H.; Wiegel, K.; Thewalt, U.; Schomburg, D. *J. Organomet. Chem.* **1975**, *87*, 301. Bürger, H., Wiegel, K. *Z. Anorg. Allg. Chem.* **1976**, *419*, 157.
(6) Olmstead, M. M.; Power, P. P.; Viggiano, M. *J. Am. Chem. Soc.* **1983**, *105*, 2927.
(7) Veith, M. *Angew. Chem., Int. Ed. Engl.* **1987**, *26*, 1; *Chem. Rev.* **1990**, *90*, 1.
(8) Heine, A.; Fest, D.; Stalke, D.; Habben, C. D.; Miller, A.; Sheldrick, G. M. *J. Chem. Soc., Chem. Commun.* **1990**, 742.
(9) Roesky, H. W.; Miller, B.; Noltemeyer, M.; Schmidt, H.-G.; Scholz, U.; Sheldrick, G. M. *Chem. Ber.* **1988**, *121*, 1403. Ergezinger, C.; Weller, F.; Dehnicke, K. *Z. Naturforsch.* **1988**, *43B* 1621. Maier, S.; Hiller, W.; Strähle, J.; Ergezinger, C.; Dehnicke, K. *Z. Naturforsch.* **1988**, *43B*, 1628. Wedler, M.; Knösel, F.; Noltemeeyer, M.; Edelmann, F. T. *J. Organomet. Chem.* **1990**, *388*, 21. Wedler, M.; Noltemeyer, M.; Pieper, U.; Schmidt, H.-G.; Stalke, D.; Edelmann, F. T. *Angew. Chem., Int. Ed. Engl.* **1990**, *29*, 941.
(10) Cloke, F. G. N.; de Lemos, H. C.; Sameh, A. A. *J. Chem. Soc., Chem. Commun.* **1986**, 1344. Rosenberger, V.; von Dieck, H. *Chem. Ber.* **1990**, *123*, 83. Bonrath, W.; Pörschke, K.; Michaelis, S. *Angew. Chem., Int. Ed. Engl.* **1990**, *29*, 298. Cloke, F. G. N.; Dalby, C. I.; Henderson, M. J.; Hitchcock, P. B.; Kennard, C. H. L.; Lamb, R. N.; Raston, C. L. *J. Chem. Soc., Chem. Commun.* **1990**, 1394.
(11) Power, P. P. *Comments Inorg. Chem.* **1989**, *8*, 177.
(12) Chen, H.; Bartlett, R. A.; Dias, H. V. R.; Olmstead, M. M.; Power, P. P. *J. Am. Chem. Soc.* **1989**, *111*, 4338.
(13) Chen, H.; Bartlett, R. A.; Olmstead, M. M.; Power, P. P.; Shoner, S. C. *J. Am. Chem. Soc.* **1990**, *112*, 1048.
(14) Evans, D. F. *J. Chem. Soc.* **1959**, 2005.
(15) Bürger, H.; Wannagat, W. *Monatsh. Chem.* **1964**, *95*, 1099.

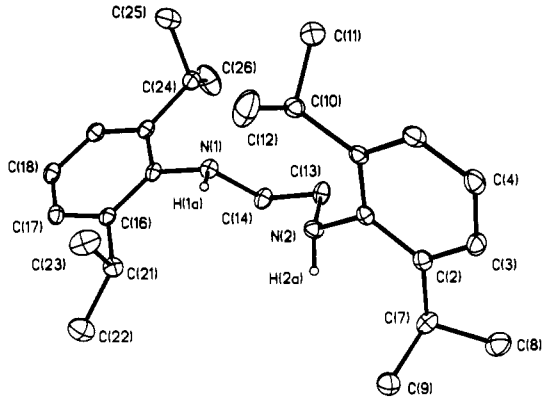

Figure 2. Thermal ellipsoidal drawing of one of the molecules of Dipp-(H)NCH_2CH_2N(H)Dipp (3). H atoms (except N H's) are omitted for clarity.

X-ray Data Collection, Solution and Refinement of the Structures. Except for compound **3**, all data were collected on a Siemens R3m/v diffractometer equipped with a locally modified Enraf-Nonius LT apparatus and all the calculations were carried out on a MicroVAX 3200 computer using SHELTXL PLUS. Data collection for compound **3** was carried out on a Syntex $P2_1$ diffractometer equipped with a locally modified Syntex LT-1 device, and the calculations were carried out by using the SHELTXL program system installed on a Data General Eclipse Series computer. The atom form factors, including anomalous scattering were from ref 16. Crystals **1** and **3–7** were transferred from the Schlenk tubes under N_2 to Petri dishes and immediately covered with a layer of hydrocarbon oil. A single crystal was selected, mounted on a glass fiber, and immediately placed in a low-temperature N_2 stream. Some details of data collection and refinement are given in Table I. Further details are provided in the supplementary material. All structures were solved by direct methods. An absorption correction (XABS) was applied. Hydrogen atoms, with the exception of N–H nitrogens, which were allowed to refine freely, were included in the refinement at calculated positions by using a riding model, with C–H of 0.96 Å and $U_H = 1.2U_C$ for compounds **1**, **3–5**, and **7** and $U_H = 1.1U_C$ for **6**. All non-hydrogen atoms were refined anisotropically except in the case of the structure of **5**, where hexane solvent C's (C(27)–C(34)) were refined isotropically, and of **7**, where C(25A) and C(26A) on one isopropyl group were refined isotropically. Selected atom coordinates and isotropic thermal parameters are given in Table II. Selected bond distances and angles are listed in Table III. The largest features on the final difference maps were 0.21, 0.18, 0.64, 0.96, 1.74, and 1.15 e/Å^3 for **1** and **3–7**, respectively. The mean shift/esd values were 0.006, 0.015, 0.002, 0.048, 0.017, and 0.068.

Structural Descriptions

$Me_2Si(NHMes)_2$ (1) and Dipp(H)NCH_2CH_2N(H)Dipp (3). The structures of **1** and **3** are illustrated in Figures 1 and 2. Both compounds crystallize as monomeric units, and there are no close interactions with neighboring molecules. The structure of **1** has a crystallographically imposed 2-fold rotation axis of symmetry and involves a central silicon atom coordinated, in a roughly tetrahedral manner, by two methyl and two NHMes groups. There is a slight flattening of the tetrahedron as indicated by the wider NSiN (116.9 (3)°) and CSiC (111.3 (4)°) angles. The nitrogen center(s) has a flattened pyramidal geometry, and the Si–N bond length is 1.723 (4) Å. There are no other structural features of unusual interest, and further details are given in Table III.

The structure of **3** possesses no crystallographically imposed symmetry. There are two crystallographically independent but chemically identical molecules in the asymmetric unit. The conformation of both molecules appears to be one which minimizes the steric interference of the large Dipp substituents. All the nitrogen centers in the molecules of **3** are pyramidal. Further important details of both structures may be found in Table III.

$[\{Li(Mes)N\}_2SiMe_2]_2$ (4) and $[Li(Dipp)NCH_2CH_2N(Dipp)Li]_2$ (5). The dilithium salts **4** and **5** both crystallize as well-separated dimers, and no close interactions with neighboring molecules are apparent in either structure. The molecules are illustrated in Figures 3 and 4. There is similarity between the cores of **4** and **5** in that they both possess what has been previously described

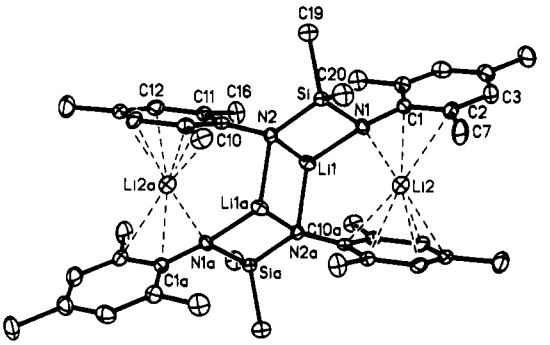

Figure 3. Thermal ellipsoidal plot of $[\{Li(Mes)N\}_2SiMe_2]_2$ (**4**). H atoms are omitted for clarity.

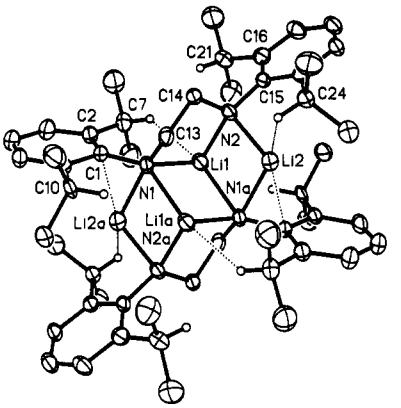

Figure 4. Thermal ellipsoidal plot of $[Li(Dipp)NCH_2CH_2N(Dipp)Li]_2$ (**5**). H atoms (except secondary H's of *i*-Pr groups) are omitted for clarity.

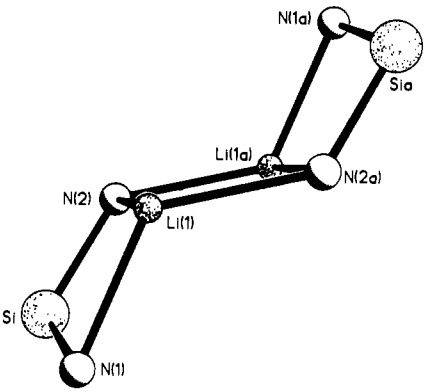

Figure 5. Drawing of the $(LiN_2Si)_2$ ladder or stair framework of **4**.

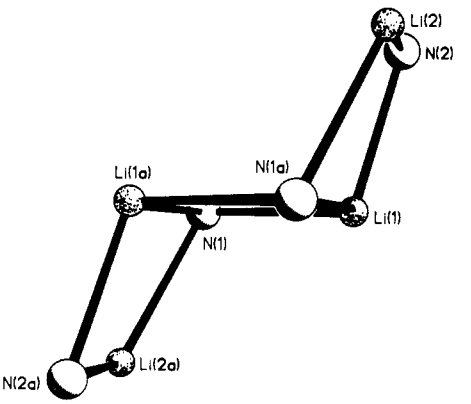

Figure 6. Drawing of the $(Li_2N_2)_2$ ladder or stair framework of **5**.

(16) *International Tables for X-ray Crystallography*; Kynoch Press: Birmingham, England, 1974; Vol. 14.

Table I. Crystallographic Data for Compounds **1** and **3–7**

	1	**3**	**4**	**5**	**6**	**7**
compd	$Me_2Si(NHMes)_2$	$DippN(H)CH_2CH_2(H)NDipp$	$[\{Li(Mes)N\}_2SiMe_2]_2$	$[Li(Dipp)NCH_2CH_2NDipp)Li]_2 \cdot {}^1/_4C_6H_{14}$	$[Li(Mn\{NMes\}_2SiMe_2)_2NSiMe_3)_2]$	$Mn[N(Dipp)CH_2CH_2N(H)Dipp]_2$
formula	$C_{20}H_{30}N_2Si$	$C_{26}H_{40}N_2$	$C_{40}H_{56}Li_4N_4Si_2$	$C_{52}H_{76}Li_4N_4 \cdot {}^1/_4C_6H_{14}$	$C_{46}H_{74}LiMn_2N_5Si_4$	$C_{52}H_{78}MnN_4$
fw	326.5	380.6	676.8	821.0	926.3	814.2
a, Å	16.401 (10)	10.968 (3)	9.360 (3)	12.758 (4)	12.918 (5)	21.713 (12)
b, Å	6.386 (2)	11.859 (4)	10.052 (2)	12.828 (5)	14.552 (5)	13.927 (6)
c, Å	9.244 (2)	20.455 (7)	11.313 (3)	19.085 (8)	13.395 (6)	17.764 (11)
α, deg		93.61 (3)	77.08 (2)			
β, deg		103.41 (3)	85.49 (2)	103.23 (2)	90.35 (3)	117.51 (2)
γ, deg		109.22 (3)	73.50 (2)			
V, Å^3	968.2 (7)	2415.5 (4)	994.7 (4)	3040 (2)	2518 (2)	4764 (4)
Z	2	4	1	4	2	4
space group	$P2_12_12$	$P\bar{1}$	$P\bar{1}$	$P2_1/c$	$P2_1$	$C2/c$
λ, Å	1.541 78	0.710 69	1.541 78	1.541 78	1.541 78	0.710 69
d(calcd), g/cm^3	1.12	1.05	1.13	0.897	1.22	1.11
μ(Cu Kα), cm^{-1}	17.5	0.56 (Mo Kα)	10.2	3.5	52.9	3.0 (Mo Kα)
range transm factors	0.88–0.93	0.98–0.99	0.80–0.91	0.72–0.78	0.13–0.23	0.92–0.96
$R(F)$	0.057	0.049	0.078	0.112	0.084	0.082
$R_w(F)$	0.080	0.050	0.090	0.122	0.093	0.109

Table II. Atomic Coordinates (×10^4) and Isotropic Thermal Parameters (Å^2 × 10^3) for the Significant Atoms in Structures **1** and **3–7**

	x	y	z	U^a		x	y	z	U^a
				Compound **1**					
Si	5000	0	6481 (2)	28 (1)	C(1)	3419 (2)	−5 (9)	7715 (5)	31 (1)
N	4193 (2)	979 (8)	7479 (5)	31 (1)	C(10)	5391 (3)	2171 (9)	5354 (6)	39 (2)
				Compound **2**					
N(1)	11924 (2)	4128 (2)	371 (1)	28 (1)	C(14)	10455 (3)	3588 (2)	132 (1)	33 (1)
N(2)	10351 (2)	2317 (2)	1026 (1)	30 (1)	C(15)	12496 (2)	5350 (2)	266 (1)	26 (1)
N(3)	1678 (2)	3479 (2)	4835 (1)	26 (1)	C(27)	−863 (3)	132 (2)	3747 (1)	25 (1)
N(4)	−449 (2)	1374 (2)	4035 (1)	25 (1)	C(39)	−228 (3)	1638 (2)	4770 (1)	28 (1)
C(1)	10243 (3)	1152 (2)	1221 (1)	25 (1)	C(40)	364 (3)	2993 (2)	4985 (1)	28 (1)
C(13)	9991 (3)	2312 (2)	282 (1)	33 (1)	C(41)	2204 (2)	4778 (2)	4879 (1)	24 (1)
				Compound **4**					
N(1)	1958 (4)	3319 (4)	6747 (3)	164 (13)	C(11)	−827 (5)	2720 (4)	3911 (4)	169 (16)
N(2)	1059 (4)	3714 (4)	4482 (3)	150 (13)	C(12)	−1605 (5)	2493 (4)	2998 (4)	208 (17)
Si	2523 (1)	2778 (1)	5408 (1)	137 (5)	C(13)	−1265 (5)	2864 (5)	1781 (4)	231 (17)
Li(1)	−58 (8)	4187 (7)	5998 (7)	176 (26)	C(14)	−53 (5)	3433 (5)	1478 (4)	234 (17)
Li(2)	1759 (9)	5044 (8)	7354 (7)	264 (30)	C(15)	779 (5)	3655 (5)	2362 (4)	182 (16)
C(1)	2527 (5)	2627 (5)	7906 (4)	167 (15)	C(19)	2911 (5)	805 (5)	5355 (4)	245 (18)
C(2)	3716 (5)	2944 (5)	8400 (4)	200 (17)	C(20)	4321 (5)	3162 (5)	4799 (5)	274 (18)
C(10)	405 (5)	3318 (4)	3604 (4)	157 (15)					
				Compound **5**					
N(1)	9705 (3)	−1001 (2)	5470 (2)	25 (1)	C(1)	9189 (3)	−1973 (3)	5552 (2)	26 (1)
N(2)	9375 (3)	1133 (2)	5981 (2)	27 (1)	C(13)	10291 (3)	−573 (3)	6180 (2)	26 (1)
Li(1)	9123 (5)	392 (5)	5069 (4)	29 (2)	C(14)	9663 (3)	265 (3)	6180 (2)	41 (2)
Li(2)	10273 (7)	1836 (6)	5434 (4)	41 (3)	C(15)	9099 (3)	2062 (3)	6311 (2)	28 (1)
				Compound **6**					
Mn(1)	3098 (2)	4214	8009 (2)	31 (1)	C(21)	188 (13)	−291 (12)	7533 (13)	48 (6)
Mn(2)	3212 (2)	2285 (2)	7670 (2)	34 (1)	C(22)	10 (11)	594 (11)	7232 (13)	43 (5)
Si(2)	3482 (4)	6473 (3)	8251 (3)	45 (1)	C(23)	572 (14)	1344 (12)	7543 (11)	47 (6)
Si(1)	1883 (3)	5742 (3)	6786 (3)	42 (1)	N(4)	4081 (9)	3479 (8)	7032 (9)	38 (4)
Si(3)	1886 (3)	2639 (3)	9519 (3)	38 (1)	C(37)	5327 (12)	2587 (13)	5479 (11)	49 (5)
Si(4)	4002 (3)	2900 (3)	5864 (3)	36 (1)	C(38)	3443 (13)	3586 (12)	4798 (13)	53 (6)
N(1)	2811 (10)	5652 (9)	7643 (8)	37 (4)	N(5)	3240 (9)	1990 (9)	6183 (9)	35 (4)
N(2)	2552 (9)	3645 (9)	9256 (9)	36 (4)	C(39)	2861 (11)	1221 (11)	5749 (10)	36 (5)
C(16)	450 (12)	2774 (13)	9768 (13)	51 (6)	C(40)	3282 (11)	343 (11)	5978 (10)	35 (5)
C(17)	2400 (15)	2140 (14)	10727 (11)	57 (6)	C(41)	2821 (11)	−469 (11)	5622 (10)	38 (5)
N(3)	2068 (9)	1953 (9)	8520 (8)	35 (4)	C(42)	1962 (12)	−478 (10)	5030 (10)	37 (5)
C(18)	1448 (11)	1200 (10)	8215 (10)	33 (4)	C(43)	1574 (13)	401 (12)	4791 (11)	43 (5)
C(19)	1719 (13)	290 (12)	8438 (11)	44 (5)	C(44)	1973 (13)	1211 (12)	5118 (11)	45 (5)
C(20)	1051 (13)	−433 (11)	8094 (14)	52 (6)	Li	1581 (19)	268 (18)	6602 (17)	36 (5)
				Compound **7**					
Mn(1)	0	647 (1)	2500	28 (1)	C(2)	−170 (3)	1399 (4)	3993 (4)	39 (3)
N(1)	309 (2)	9 (3)	3622 (3)	31 (2)	C(3)	544 (3)	−936 (4)	3917 (4)	31 (2)
N(2)	−155 (2)	1937 (3)	3286 (3)	29 (2)	C(15)	−575 (3)	2799 (4)	3093 (4)	34 (2)
C(1)	395 (3)	639 (4)	4312 (3)	41 (3)					

[a] Equivalent isotropic U defined as one-third of the trace of the orthogonalized U_{ij} tensor.

as a "ladder" structure. For **4** the ladder is composed of two attached Li(1)N(1)SiN(2) rings that are related through an inversion center (Figure 5). In **5**, however, the ladder is derived from two Li_2N_2 rings that are also related by a center of inversion (Figure 6). (In view of the zigzag nature of the $(Li–N)_2$ or $(LiSiN_2)$ rings in the structure of **4** and **5**, an analogy between these frameworks and stairs may be more apt.) The interplanar angle between the four-membered rings in the backbone of **4** is

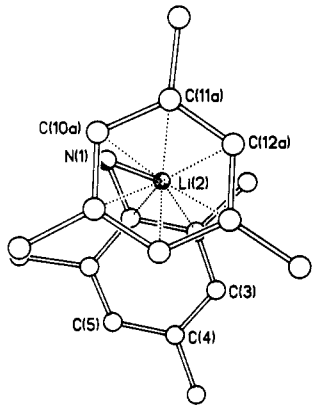

Figure 7. Drawing illustrating the coordination environment of the Li(2) atom in **4**.

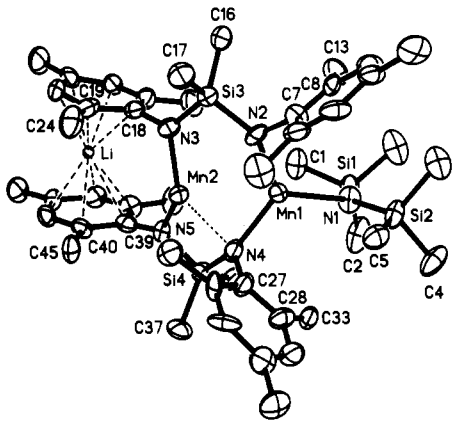

Figure 8. Thermal ellipsoidal plot of $[Li(Mn\{NMes\}_2SiMe_2)_2N(SiMe_3)_2]$ (**6**). H atoms are omitted for clarity.

129.6° and in **5** it is 107.5°. The primary coordination of the lithium atoms in **5** is to the nitrogen centers, and the Li–N distances are in the range 1.940 (9)–2.146 (8) Å. In addition, there are some very close approaches between Li(1), Li(2), and various carbon and hydrogens from the Dipp group: for example, Li(2)–C(1a) = 2.153 (10) Å, Li(2)–H(24a) = 2.24 Å, and Li(1)–H(7a) = 2.24 Å.

In **4**, the Li(1) atoms are coordinated by three nitrogen atoms, which gives rise to trigonal pyramidal coordination for these metals. The Li(2) and Li(2a) centers, however, are bound to one nitrogen only, and the Li–N bond length is 1.96 (1) Å. In addition, the outer lithiums have close interactions with various carbons from the mesityl rings. For example Li(2) is located directly over the centroid of the C(10a) mesityl ring as illustrated in Figure 7. The average Li(2)–C(ring) distance is nearly 2.39 Å. In addition, Li(2) apparently interacts with the C(1) and C(2) from the C(1) mesityl ring, and these corresponding distances are 2.82 (9) and 2.98 (9) Å. Another notable structural feature is the 7.8° angle between the N(2)–C(10a) bond and the C(10a) ring plane.

$[Li(Mn\{N(Mes)\}_2SiMe_2)_2N(SiMe_2)_2]$ (6). The unusual structure, Figure 8, exhibited by compound **6** involves molecular units in which the dinegative $[(NMes)_2SiMe_2]^{2-}$ ligand bridges two dissimilar Mn(II) centers. The Mn(1)···Mn(2) separation is 2.848 (3) Å. The difference in the metal centers mainly arises from the inclusion of the ligand $[N(SiMe_3)_2]^-$ in the coordination sphere of Mn(1). The Mn(1) atom has three-coordinate planar coordination with Mn(1)–N distances in the range 1.93 (1)–2.18 (1) Å. The coordination sphere at Mn(2) involves two short bonds of 1.93 (1) and 2.04 (1) Å to N(3) and N(5). There is a further possible interaction with N(4) since the Mn(2)···N(4) distance is 2.24 (1) Å. The geometry at N(4), however, is calculated to be almost planar since the sum of the angles Mn(1)–N(4)–C(27), C(27)–N(4)–Si(4), and Si(4)–N(4)–Mn(1) is 358.1°. In addition, a hydrogen atom located on C(36) is calculated to be 1.83 Å distant from Mn(2). The sum of the angles at Mn(2) (including

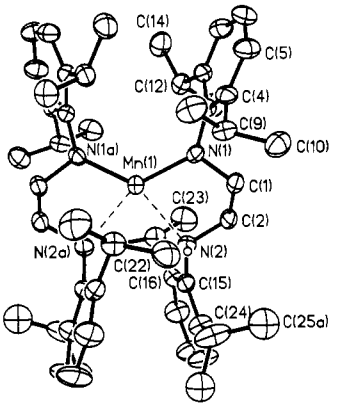

Figure 9. Thermal ellipsoidal plot of $Mn[N(Dipp)CH_2CH_2N(H)Dipp]_2$ (**7**). H atoms (except N H's) are omitted for clarity.

N(4) in the coordination sphere) is 344.1° so that the Mn(2) center in the three-coordinate environment has significant pyramidal character.

The structure of **6** is completed by the inclusion of a Li^+ ion sandwiched between the planes of the C(18) and C(39) mesityl rings. These rings are not parallel, however, and there is an angle of 7.6° between their planes. The Li–C distances are in the range 2.25–2.56 Å and average 2.40 Å. The average C–C distances within the C(18) and C(39) rings are 1.399 (34) and 1.396 (24) Å, and there is no significant difference between these and the average values observed in the C(7) (1.389 (30) Å) and the C(27) (1.424 (25) Å) rings.

$Mn[N(Dipp)CH_2CH_2NHDipp]_2$ (7). The crystal structure of **7** consists of discrete mononuclear units of the title formula and is illustrated in Figure 9. It possesses a crystallographically imposed 2-fold rotation axis of symmetry through the Mn atom. The manganese center is four-coordinate with two short, Mn(1)–N(1) = 1.992 (5) Å, bonds and two much longer, Mn(1)–N(2) = 2.394 (5) Å, interactions. The amido nitrogen centers have a three-coordinate, almost planar geometry, as indicated by $\sum°N(1)$ being equal to 359.6 (4)° whereas the amine nitrogens, which retain their hydrogens, have a very distorted tetrahedral coordination. The angles surrounding the metal center indicate a geometry that is nearer to planarity than it is to tetrahedral. The N(1)–Mn–N(1a) angle is 127.1 (3)° whereas the N(2)–Mn–N(2a) angle is 82.4 (3)°. The angle between the MnN(1)N(2) and MnN(1a)N(2a) planes is 35.4°.

Discussion

The bidentate ligand precursors **1–3** were synthesized by straightforward procedures as indicated by eqs 1 and 2. The

$$2LiNHMes + Me_2SiCl_2 \rightarrow \underset{\mathbf{1}}{Me_2Si(NHMes)_2} + 2LiCl \quad (1)$$

$$\text{excess } ArNH_2 + BrCH_2CH_2Br \rightarrow [Ar(H)_2NCH_2CH_2N(H)_2Ar]^{2+}[Br]^-_2 \xrightarrow{KOH} Ar(H)NCH_2CH_2N(H)Ar + 2KBr + H_2O \quad (2)$$

Ar = Mes (**2**), Dipp (**3**)

synthesis of **1**, which is based on well-known Si–N chemistry, proceeded smoothly and in high yield. The synthesis of **2** and **3** was adapted from a general procedure[17] for the synthesis of multidentate amine compounds. The bidentate amines **1–3** are among the bulkiest now known. This is especially true in the case of **3**, and initial experiments in this laboratory have concentrated on this species rather than the related, but less bulky, **2**. Presumably, the size of the ligand **1** could be further augmented by using H_2NDipp to obtain the, as yet unreported, species $Me_2Si\{N(H)Dipp\}_2$. The structures of **1** and **3** need no further comment here except to note that they were undertaken, primarily to obtain data for later comparison with their metal derivatives.

(17) Barefield, E. K.; Wagner, F. W.; Herlinger, A. M.; Dahl, A. R. *Inorg. Synth.* **1976**, *16*, 220.

Table III. Selected Bond Distances (Å) and Angles (deg) for Compounds 1 and 3–7

Compound 1					
Si–N	1.730 (4)	N–C(1)	1.433 (6)	Si–C(10)	1.849 (6)
N–H	0.85 (8)				
N–Si–N(a)	115.6 (3)	N–Si–C(10a)	107.8 (2)	C(10)–Si–N(a)	107.8 (2)
C(10)–Si–C(10a)	111.4 (4)	Si–N–H	106 (4)	H–N–C(1)	115 (4)
Compound 3[a]					
N(1)–C(14)	1.470 (4)	N(1)–C(15)	1.429 (3)	N(2)–C(1)	1.438 (3)
N(2)–C(13)	1.479 (3)	N(1)–H(1a)	0.84 (2)	N(2)–H(2a)	0.87 (3)
C(14)–N(1)–C(15)	115.1 (2)	C(14)–N(1)–H(1a)	106.5 (1.5)	C(15)–N(1)–H(1a)	109.9 (1.4)
C(1)–N(2)–C(13)	115.6 (2)	C(1)–N(2)–H(2a)	109.8 (1.9)	C(13)–N(2)–H(2a)	108.2 (1.8)
N(2)–C(1)–C(6)	119.2 (2)	N(2)–C(13)–C(14)	109.3 (2)	N(1)–C(14)–C(13)	109.9 (2)
N(1)–C(15)–C(16)	119.8 (2)	N(1)–C(15)–C(20)	119.2 (2)		
Compound 4					
N(1)–Si	1.717 (4)	N(2)–Si	1.707 (3)	N(1)–Li(2)	1.96 (1)
N(1)–Li(1)	2.007 (8)	Li(1)–N(2)	2.015 (8)	Li(1a)–N(2)	2.017 (7)
Li(2)–C(1)	2.282 (9)	Li(2)–C(2)	2.498 (9)	Li(2)–C(10a)	2.375 (8)
Li(2)–C(11a)	2.347 (8)	Li(2)–C(12a)	2.382 (9)	Li(2)–C(13a)	2.43 (1)
Li(2)–C(14a)	2.413 (9)	Li(2)–C(15a)	2.400 (9)	N(1)–C(1)	1.407 (5)
N(2)–C(10)	1.390 (6)				
N(1)–Si–N(2)	102.5 (2)	N(1)–Si–C(19)	114.0 (2)	N(1)–Si–C(20)	112.7 (2)
N(2)–Si–C(19)	111.8 (2)	N(2)–Si–C(20)	112.4 (2)	C(19)–Si–C(20)	103.8 (2)
Li(1)–N(2)–Li(1a)	76.2 (3)	N(2)–Li(1)–N(2a)	103.8 (3)	N(1)–Li(1)–N(2)	83.2 (3)
N(1)–Li(1)–N(2a)	125.3 (5)	C(10)–N(2)–Li(1a)	96.4 (3)		
Compound 5					
Li(1)–N(1)	2.018 (7)	Li(1)–N(1a)	2.146 (8)	Li(1)–N(2)	1.945 (7)
Li(2)–N(2)	1.940 (9)	N(1)–C(1)	1.436 (5)	N(1)–C(13)	1.495 (5)
N(2)–C(15)	1.430 (5)	N(2)–C(14)	1.462 (5)	Li(2a)–N(1)	2.036 (9)
Li(2)···C(1a)	2.15 (1)	Li(2)···C(15)	2.51 (1)	Li(2)···H(24a)	2.24
Li(1)···H(7a)	2.24				
N(1)–Li(1)–N(1a)	105.5 (3)	N(1)–Li(1)–N(2)	97.0 (3)	Li(1)–N(2)–Li(2)	75.1 (3)
Li(1)–N(1)–Li(1a)	74.5 (3)	N(2)–Li(1)–N(1a)	105.1 (3)	Li(1a)–N(1)–Li(2a)	68.9 (3)
C(1)–N(1)–C(13)	111.5 (3)	N(1)–C(1)–C(2)	120.4 (3)	N(1)–C(1)–C(6)	121.0 (4)
N(1)–C(13)–C(14)	113.9 (3)	N(2)–C(14)–C(13)	111.0 (3)	N(2)–C(15)–C(16)	120.5 (3)
N(2)–C(15)–C(20)	120.6 (4)				
Compound 6					
Mn(1)···Mn(2)	2.848 (3)	Mn(1)–N(1)	2.18 (1)	Mn(1)–N(2)	2.00 (1)
Mn(1)–N(4)	2.12 (1)	Mn(2)–N(3)	1.93 (1)	Mn(2)···N(4)	2.24 (1)
Mn(2)–N(5)	2.04 (1)	Li–C(18)	2.56 (3)	LiC(19)	2.57 (3)
Li–C(20)	2.35 (3)	Li–C(21)	2.34 (3)	Li–C(22)	2.25 (3)
Li–C(23)	2.40 (3)	Li–C(39)	2.45 (3)	Li–C(40)	2.36 (3)
Li–C(41)	2.34 (3)	Li–C(42)	2.42 (3)	Li–C(43)	2.43 (3)
Li–C(44)	2.47 (3)	N(1)–Si(1)	1.66 (1)	N(1)–Si(2)	1.68 (1)
N(2)–Si(3)	1.74 (1)	N(3)–Si(3)	1.69 (1)	N(4)–Si(4)	1.78 (1)
Si(4)–N(5)	1.706 (13)				
N(1)–Mn(1)–N(2)	121.7 (5)	N(1)–Mn(1)–N(4)	116.6 (4)	N(2)–Mn(1)–N(4)	121.6 (5)
N(3)–Mn(2)···N(4)	143.6 (5)	N(3)–Mn(2)–N(5)	122.8 (5)	N(4)···Mn(2)–N(5)	77.2 (5)
Mn(1)–N(2)–Si(3)	134.3 (7)	N(2)–Si(3)–N(3)	105.4 (6)	Mn(2)–N(3)–Si(3)	115.5 (7)
Mn(1)–N(4)···Mn(2)	81.5 (4)	C(16)–Si(3)–C(17)	103.2 (8)	N(4)–Si(4)–N(5)	100.2 (6)
C(37)–Si(4)–C(38)	105.7 (7)				
Compound 7					
Mn(1)–N(1)	1.994 (5)	Mn(1)···N(2)	2.393 (6)	N(1)–C(1)	1.448 (8)
N(1)–C(3)	1.422 (7)	N(2)–C(2)	1.476 (9)	N(2)–C(15)	1.451 (7)
N(2)–H(1)	0.86 (8)				
N(1)–Mn(1)–N(1a)	127.1 (3)	N(2)–Mn(1)–N(2a)	82.4 (3)	N(1)–Mn(1)–N(2)	79.9 (3)
N(2)–Mn(1)–N(1a)	147.6 (3)	Mn(1)–N(1)–C(1)	115.4 (4)	Mn(1)–N(1)–C(3)	132.8 (4)
C(1)–N(1)–C(3)	111.4 (5)				

[a] Values are from one molecule only; the other molecule is very similar.

The Lithium Salts 4 and 5. The lithiation of **1** and **3** proceeded smoothly and in high yield to give **4** and **5** as illustrated by eqs 3 and 4. The structures of **4** and **5** have little precedent among the handful that are currently known for polylithiated compounds.

$$2Me_2Si(NHMes)_2 + 4\,n\text{-BuLi} \rightarrow \underset{\mathbf{4}}{[\{Li(Mes)N\}_2SiMe_2]_2} + 4\,n\text{-BuH} \quad (3)$$

$$2Dipp(H)NCH_2CH_2N(H)Dipp + 4\,n\text{-BuLi} \rightarrow \underset{\mathbf{5}}{[Li(Dipp)NCH_2CH_2N(Dipp)Li]_2} + 4\,n\text{-BuH} \quad (4)$$

The ladder[18] or stair frameworks seen in **4** and **5** are indeed similar to those observed in monolithiated amide compounds such as $[H_2C(CH_2)_3NLi]\cdot MeN(CH_2CH_2NMe_2)_2$.[19] However, neither **4** nor **5** is complexed by solvent molecules or other donors. In addition, the structure of the dilithium solvate salt [{Li(Ph)-

(18) Armstrong, D. R.; Barr, D.; Clegg, N.; Mulvey, R. E.; Read, D. R.; Snaith, R.; Wade, K. *J. Chem. Soc., Chem. Commun.* **1986**, 869. Clegg, W.; Snaith, R.; Wade, K. *Inorg. Chem.* **1988**, *27*, 3861.
(19) Armstrong, D. R.; Barr, D.; Brooker, A. T.; Clegg, W.; Gregory, K.; Hodgson, S. M.; Snaith, R.; Wright, D. S. *Angew. Chem., Int. Ed. Engl.* **1990**, *29*, 410.

$NCH_2CH_2N(Ph)Li\}\cdot 3HMPA]$[18] does not resemble those of **4** and **5**. Instead it possesses a monomeric structure with two lithium centers that doubly bridge the two nitrogens. The lithium coordination is completed by a terminal and bridging HMPA molecule. There is some resemblance between the structure of **4** and that of $[Et_2OLi\{(t\text{-}Bu)N\}_2SiMe]_2$,[20] which has a ladder (stair) structure that is derived from two LiN_2Si rings. However, it is notable that the latter compound is not a polylithiated compound in the sense that **4** is.

Not surprisingly, many of the Li–N bonds in both **4** and **5** are quite short. The shortest Li–N distances in **4** and **5** are 1.96 (1) and 1.940 (9) Å. In both of these cases, the nominal coordination number of lithium is low. Thus, in **4**, Li(2) is bound only to N(1) and the π-orbitals of the C(1) and C(10a) rings, and in **5**, Li(2) is bound to two nitrogens and has further interactions with the C(1a) ring and possibly H(24a). Nonetheless, these Li–N bonds are not as short as the Li–N distance of 1.895 (8) Å in the complex $[(TMEDA)LiNH(2,4,6\text{-}t\text{-}Bu_3C_6H_2)]$.[21] In this species the Li center is three-coordinate and bound to σ-bonding ligands. On the basis of these data, it is possible to argue that the Li–N distances in **4** and **5** are somewhat longer than expected. The relative length of these Li–N bonds testifies to the strength of the nonclassical interactions with the other groups within these molecules. Thus, in **4**, the most remarkable feature of the structure is the interaction between Li(2) and eight ring carbons. The Li(2)–C distances can vary from 2.28 to 2.5 Å and average about 2.39 Å. In view of the high effective coordination number of lithium, the average Li–C distance may be regarded as being indicative of significant bonding. This view is reinforced by the observation of a 7.8° angle between N(2)–C(10) and the C(10) ring plane, which suggests that the aromatic ring is strongly attracted by the lithium ion. The Li–C bonds are, in fact, not a great deal shorter than the 2.40-Å Li–C distance in the compound $[Li(indenofluorenyl)]_2$,[22] which features two lithium ions sandwiched between two η^6 π systems. Significant though these nonclassical interactions are, they are not as strong as the very short Li(2)C(1a) distance, 2.15 (1) Å, observed in **5**. This distance is comparable to those observed in many organolithium compounds. For example, it is far shorter than the 2.33 Å observed in $[Li(Et_2O)Ph]_4$[23] or the 2.203 (3) and 2.249 (3) Å seen in $[Li(Et_2O)2,4,6\text{-}i\text{-}Pr_3C_6H_2]_2$.[24]

A few other structural features of **4** and **5** merit comment. The N–Si distances in **4**, average 1.712 (5) Å, are marginally shorter than those in **1**. This is a characteristic of metal silylamides and is probably a result of the increased ionic interaction between N and Si as a result of the substitution of H by Li. In structure of **3** the N–C(aromatic) bonds are about 0.04 Å shorter than the N–C(aliphatic) bonds. In the dilithium salt **5**, there is no observable change in the N–C bond lengths as a result of the substitution of H by Li. The lack of bond contraction in the case of **5** could be a result of greater covalency of the N–C bond, which may not be as strongly affected by ionic factors as the more polar N–Si link.

The Manganese Compounds 6 and 7. The unusual stoichiometry of compound **6** arose from the fortuitous inclusion of $LiN(SiMe_3)_2$ in what was thought to be a pure sample of $Mn[N(SiMe_3)_2]_2$.[15] The reaction of this mixture with the ligand **1** afforded the product **6** in moderate yield as illustrated by eq 5. The starting Mn species

$$2Me_2Si(NHMes)_2 + 2Mn[N(SiMe_3)_2]_2 \xrightarrow{LiN(SiMe_3)_2} [Li(Mn\{NMes\}_2SiMe_2)_2N(SiMe_3)_2] + 2HN(SiMe_3)_2 \quad (5)$$

was prepared by the reaction of $LiN(SiMe_3)_2$ with $MnBr_2$.[15] The reaction, which usually affords pure $Mn[N(SiMe_3)_2]_2$, may have had some unreacted $LiN(SiMe_3)_2$ as part of the product, which distilled along with the manganese amide. In addition, it is possible that a species such as $LiMn\{N(SiMe_3)_2\}_3$, in an unsolvated or in an ether-solvated form, may be part of the contaminant. The latter type of species has been observed as a product during the reaction between $MnBr_2$ and $LiN(SiMe_3)_2$, and it has been structurally characterized as the THF adduct $[(THF)LiMn\{N(SiMe_3)_2\}_3]$.[25] These caveats notwithstanding, the reaction may be performed in a rational manner in accordance with the stoichiometry in eq 5 by using pure $Mn[N(SiMe_3)_2]_2$ and $LiN(SiMe_3)_2$.

The bonding of the $N(SiMe_3)_2$ ligand to Mn(1) in the structure of **6** gives rise to two different coordination environments at the manganese centers. The inclusion of Li^+ sandwiched between the C(18) and C(39) aromatic rings imposes further distortions on the structure, especially at Mn(2). Clearly, the Mn(1) center has a three-coordinate planar coordination, and the Mn–N bond distances 1.93 (1)–2.18 (1) Å (average ~2.1 Å) are essentially the same as those observed in $[(THF)LiMn\{N(SiMe_3)_2\}_3]$ (average 2.1 Å). The description of the coordination at Mn(2) is not quite as clear-cut. In this case, there are two short Mn–N bonds, which average 1.985 Å in length, and one longer Mn–N interaction of 2.24 (1) Å with N(4). The short Mn–N distance corresponds very closely to the 1.989 (3) Å measured in the two-coordinate Mn species $Mn\{N(SiMePh_2)_2\}_2$.[12] In addition, it has already been noted that the N(4) center has a geometry that is very close to planarity. These data indicate that the interaction between Mn(2) and N(4) is probably quite weak, and as a result, the geometry may be more accurately described as two-coordinate. Inspection of the illustration in Figure 8 shows that the Li^+ ion is sandwiched between the two aromatic rings on the opposite side of Mn(2) from N(4). A likely explanation for the bending of the N(3)–Mn(2)–N(5) angle toward N(4) is that the Li^+ coordination pulls the aromatic rings toward each other. The consequent ring separation is inconsistent with a linear coordination at Mn(2) so that the observed bent coordination is the result.

Sandwich compounds involving the Li^+ ion are quite rare. In terms of the Li^+ coordination, the structure of **6** is similar to that previously mentioned species $[Li(indenofluorenyl)]_2$. However, the C(18) and C(39) rings in **6** are not quite parallel and have an interplanar angle of 7.6°. The Li^+ ion is located over the centroid of each ring, and the Li–C interactions average 2.4 Å, which is the same as the average Li–C bond length seen in $[Li(indenofluorenyl)]_2$.[22] This supports the view that the Li^+ coordination in **6** is quite energetically significant and that **6** is not merely a weak inclusion complex.

The distance between the metals in **6** is 2.848 (3) Å, which is indicative of little or no Mn–Mn bonding. Nonetheless, the low value for the magnetic moment, 2.9 μ_B, suggests that there is considerable antiferromagnetic coupling between the two Mn(II) centers that are presumably high spin.

The reaction between $Mn[N(SiMe_3)_2]_2$ and the ligand **3** results in the isolation of **7** as illustrated by eq 6. The structure of the

$$2Dipp(H)NCH_2CH_2N(H)Dipp + Mn[N(SiMe_3)_2]_2 \rightarrow 2HN(SiMe_3)_2 + Mn[N(Dipp)CH_2CH_2N(H)Dipp]_2 \quad (6)$$

product **7** features high-spin Mn^{2+} bonded to two $[NDippCH_2CH_2N(H)Dipp]^-$ ligands. The ligands are bound primarily as amide groups. The Mn(1)–N(1) bond length is 1.994 (5) Å, which is close to that previously observed in a two-coordinate Mn(II) amide.[11-13] The other Mn–N(2) interaction, to the amine end of the amide ligand, is 2.393 (6) Å, which is 0.4 Å longer than the Mn–N(1) distance. Since the radius of an Mn atom is estimated to be about 1.39 Å[26] and the radius of nitrogen is about 0.70–0.73 Å, an average value for an Mn–N bond is then calculated to be 2.09–2.12 Å. Clearly, then, the interaction between Mn(1) and N(2) is quite weak since it is 0.28 Å longer than this value. The Mn(1) center is thus quasi-two-coordinate. The

(20) Veith, M.; Goggin, F.; Huch, V. *Chem. Ber.* **1988**, *121*, 943.
(21) Fjelberg, T.; Hitchcock, P. B.; Lappert, M. F.; Thorne, A. T. *J. Chem. Soc., Chem. Commun.* **1984**, 822.
(22) Bladauski, D.; Broser, W.; Hecht, H.-J.; Rewicki, D.; Dietrich, H. *Chem. Ber.* **1979**, *112*, 1380.
(23) Hope, H.; Power, P. P. *J. Am. Chem. Soc.* **1983**, *105*, 5320.
(24) Bartlett, R. A.; Dias, H. V. R.; Power, P. P. *J. Organomet. Chem.* **1988**, *341*, 1.
(25) Murray, B. D.; Power, P. P. *Inorg. Chem.* **1984**, *23*, 4584.
(26) Covalent radii estimated from homonuclear bond lengths: Sutton, L., Ed. *Tables of Interatomic Distances and Configuration in Molecular and Ions*, Special Publication—Chemical Society 11 and 18; Chemical Society: London, 1958 and 1965. See also ref 11, p 20.

overall configuration at the Mn(1) center is also remarkable. Both the amide bonds are on one side of the manganese (cis) with an angle of 127.1 (3)° between them. This unusual coordination is, in some respects, reminiscent of the coordination seen in the metal borylamides $M(NArBMes_2)_2$ (M = Cr-Ni; Ar = Ph or Mes).[11,13,12][7] The metal coordination in these molecules is also 2-fold, but secondary interactions are observed between the metal and an ipso carbon of a boron-mesityl group so that cis structures very similar to that seen in **7** are observed. This is especially true for the Cr and Mn complexes. Another interesting feature of this structure is that if the weak coordination to N(2) is taken into account, the resulting four-coordinate structure is closer to planar coordination than it is to tetrahedral coordination. This is because the angle between the Mn(1)N(1)N(2) and Mn(1)N(1a)N(2a) planes is only 35.4°. This observation is difficult to explain since the structure is quite crowded. This crowding is evident in the bending of the aromatic rings away from each other. For example, there is an angle of 8.2° between the N(1)-C(3) bond and the plane of the C(3) phenyl ring, and an angle of 5.5° is observed between the N(2)-C(15) bond and the C(15) ring plane. This congestion might have been relieved by the adoption of a trans geometry at Mn(1) or by dispensing with the coordination of one or both of the N(2) atoms. The structure of **7** is apparently a comprise between these competing factors. Experiments on these and related ligands and their transition-metal complexes is continuing.

Acknowledgment. We thank the donors of the Petroleum Research Fund, administered by the American Chemical Society, for support of this work.

Supplementary Material Available: Tables giving full details of X-ray data collection and refinement and complete atom coordinates, bond distances and angles, hydrogen coordinates, and anisotropic thermal parameters and a drawing of the second molecule of **3** in the asymmetric unit (34 pages). Ordering information is given on any current masthead page.

(27) Bartlett, R. A.; Chen, H.; Power, P. P. *Angew. Chem., Int. Ed. Engl.* **1989**, *28*, 316.

Contribution from the Department of Chemistry, Baker Laboratory, Cornell University, Ithaca, New York 14853

Pyridine and Related Adducts, $(silox)_3ML$ (M = Sc, Ti, V, Ta): η^1-Pyridine-*N* vs η^2-Pyridine-*N*,*C* Ligation

Katharine J. Covert, David R. Neithamer, Marjanne C. Zonnevylle, Robert E. LaPointe, Christopher P. Schaller, and Peter T. Wolczanski*,†

Received October 29, 1990

Adducts of $(silox)_3M$ (M = Ta (**1**), Ti (**2**), Sc (**3**), V (**4**)) have been prepared in order to assess the various electronic factors responsible for η^1-pyridine-*N* vs. η^2-pyridine-*N*,*C* ligation. Treatment of $ScCl_3(THF)_3$ or VCl_3 with 3 equiv of Na(silox) in THF yielded $(silox)_3M(THF)$ (M = Sc (**3**-THF), V (**4**-THF)), and exposure of $[(Me_3Si)_2N]_3Sc$ to 5 equiv of (silox)H provided $(silox)_3ScNH_3$ (**3**-NH_3), but the bases could not be removed. Addition of C_2H_4, C_2H_3Me, 1-butene, and *cis*-2-butene to **1** afforded $(silox)_3Ta(olefin)$ (olefin = C_2H_4 (**5a**), C_2H_3Me (**5b**), C_2H_3Et (**5c**), *cis*-MeHC=CHMe (**5d**)), although cyclometalation to give $(silox)_2HTaOSi^tBu_2CMe_2CH_2$ (**6**) competed with the latter two. In concentrated benzene solution (~0.10 M), **1** trapped C_6H_6 to yield $[(silox)_3Ta]_2\{\mu\text{-}\eta^2(1,2):\eta^2(4,5)\text{-}C_6H_6\}$ (**7**; ~7%) along with **6**. Acetylene, 2-butyne, and $F_3CC{\equiv}CCF_3$ reacted with **1** to give $(silox)_3Ta(alkyne)$ (alkyne = C_2H_2 (**8a**), C_2Me_2 (**8b**), $C_2(CF_3)_2$ (**8c**)). Ethylene did not displace the THF and NH_3 from **3**-THF, **3**-NH_3, and **4**-THF, but reacted with **2** to provide $[(silox)_3Ti]_2(\mu\text{-}C_2H_4)$ (**9**). Treatment of **1** with pyridine, 2-picoline, 2,6-lutidine, pyridazine ($1,2\text{-}N_2C_4H_4$) and pyrimidine ($1,3\text{-}N_2C_4H_4$) provided $(silox)_3Ta(\eta^2\text{-}NC_5H_5\text{-}N,C)$ (**10a**), $(silox)_3Ta(\eta^2\text{-}6\text{-}NC_5H_4Me\text{-}N,C)$ (**10b**), $(silox)_3Ta(\eta^2\text{-}2,6\text{-}NC_5H_3Me_2\text{-}N,C)$ (**11b**), $(silox)_3Ta(\eta^2\text{-}N_2C_4H_4\text{-}N,N')$ (**12**), and $(silox)_3Ta(\eta^2\text{-}1,3\text{-}N_2C_4H_4\text{-}N^1,C^6)$ (**13**), respectively. Formation of these η^2-heterocyclic adducts is proposed to occur via nucleophilic attack by **1** at the LUMO (predominantly C=N π^*) of the substrate, a process consistent with the generation of the pyridyl hydride $(silox)_3Ta(H)(C_5H_2Me_2N)$ (**11a**) from 2,6-lutidine prior to equilibration with **11b**. Similar treatments of **2** yielded $(silox)_3Ti(\eta^1\text{-py})$ (**2**-py) and related η^1-py derivatives of 3,5-lutidine (**2**-3,5-$NC_5H_3Me_2$), 4-picoline (**2**-4-NC_5H_4Me), and 4-$NC_5H_4{}^tBu$ (**2**-4-$NC_5H_4{}^tBu$). Upon application of the McConnell equation to a_H values obtained from the ^1H contact shifts of **2**-py, the following spin density probabilities were obtained: $\rho^2(2,6) = 0.13\%$; $\rho^2(3,5) = 0.01\%$; $\rho^2(4) = 0.16\%$. η^1-Pyridine adducts $(silox)_3M(py)$ (M = Sc (**3**-py), V (**4**-py)) were produced upon exposure of $(silox)_3M(THF)$ to py. Interpretation of the UV-vis spectrum of **1** and EHMO calculations of η^1 and η^2 forms of $(silox)_3Ta(py)$ provide a rationale for the variation in pyridine ligation. Of critical importance are the four-electron repulsion between the filled d_{z^2} orbital of **1** and the py N-donor orbital and the capability of pyridine to function as a good π-acceptor in the η^2-mode.

Introduction

σ-Interactions dominate the bonding in organotransition-metal complexes, but π-effects are significant, especially in complexes containing carbon-based ligands that possess a degree of unsaturation.[1] Through the use of molecular orbital theory,[2] π-interactions in organometallic complexes can be rationalized, and the bonding of complicated ligand systems can be cogently analyzed and understood. While theory has provided a basis for examining π-effects, disclosures of unusual bonding modes still provide the field of organometallics with some of its most interesting chemistry. Recently, investigations of η^2-arene complexes[3-13] have played an important role in determining the mechanisms of arene C-H bond activations.[8,9,14,15] In addition, structural and molecular orbital studies of tantalum arene complexes revealed that even the hapticity of hexasubstituted benzenes is moot;[16-18] consequently, 7-metallanorbornadienes have been proposed as intermediates in the cyclotrimerization of alkynes.[16] These and

† Alfred P. Sloan Foundation Fellow, 1987-1989.

(1) (a) Collman, J. P.; Hegedus, L. S.; Norton, J. R.; Finke, R. G. Principles *and Applications of Organotransition Metal Chemistry*; University Science Books: Mill Valley, CA, 1987. (b) Yamamoto, A. *Organotransition Metal Chemistry*; Wiley Interscience: New York, 1986. (c) Crabtree, R. *The Organometallic Chemistry of the Transition Metals*; Wiley Interscience: New York, 1988. (d) Elschenbroich, Ch.; Salzer, A. *Organometallics*; VCH Publishers: New York, 1989.
(2) For examples, see: (a) Hoffmann, R. *Angew. Chem., Int. Ed. Engl.* **1982**, *21*, 711-724. (b) Albright, T. A. *Tetrahedron* **1982**, *38*, 1339-1388 and references therein.
(3) Muetterties, E. L.; Bleeke, J. R.; Wucherer, E. J.; Albright, T. A. *Chem. Rev.* **1982**, *82*, 499-525.
(4) Jonas, K. *Angew. Chem., Int. Ed. Engl.* **1985**, *24*, 295-311.
(5) Jonas, K.; Wiskamp, V.; Tsay, Y.-H.; Krüger, C. *J. Am. Chem. Soc.* **1983**, *105*, 5480-5481.
(6) (a) Gomez-Sal, M. P.; Johnson, B. F. G.; Lewis, J.; Raithby, P. R.; Wright, A. H. *J. Chem. Soc., Chem. Commun.* **1985**, 1682-1684. (b) Deeming, A. J. *Adv. Organomet. Chem.* **1986**, *26*, 1-83.

0020-1669/91/1330-2494$02.50/0